https://doi.org/10.5194/acp-2023-47
Preprint. Discussion started: 17 April 2023

Atmospheric Chemistry and Physics Discussions

Rapid assimilations of O_3 observations – Part 2: tropospheric O_3 changes in the United States and Europe in 2005-2020

Rui Zhu[1], Zhaojun Tang[1], Xiaokang Chen[1], Zhe Jiang[1]* and Xiong Liu[2]

[1]School of Earth and Space Sciences, University of Science and Technology of China, Hefei, Anhui, 230026, China.
[2]Center for Astrophysics | Harvard & Smithsonian, Cambridge, MA 02138, USA.

*Correspondence to: Zhe Jiang (zhejiang@ustc.edu.cn)

Abstract

Tropospheric nitrogen dioxide (NO_2) concentrations have declined dramatically over the United States (US) and Europe in recent decades. Here we investigate the changes in surface and free tropospheric O_3 associated with NO_2 changes over the US and Europe in 2005-2020 by assimilating the Ozone Monitoring Instrument (OMI), and US Air Quality System (AQS) and European AirBase network O_3 observations. The assimilated O_3 concentrations demonstrate good agreement with O_3 observations: surface O_3 concentrations are 41.4, 39.5 and 39.5 ppb (US) and 35.3, 32.0 and 31.6 ppb (Europe); and tropospheric O_3 columns are 35.5, 37.0 and 36.8 DU (US) and 32.8, 35.3 and 36.4 DU (Europe) in the simulations, assimilations and observations, respectively. We find overestimated summertime surface O_3 concentrations over the US and Europe, which resulted in a surface O_3 maximum in July-August in simulations in contrast to April in observations. Furthermore, our analysis exhibits limited changes in surface O_3 concentrations, i.e., decreased by -6% over the US and increased by 1.5% over Europe in 2005-2020. The surface observation-based assimilations suggest insignificant changes in tropospheric O_3 columns: -3.0% (US) and 1.5% (Europe) in 2005-2020. While the OMI-based assimilations exhibit larger decreases in tropospheric O_3 columns, -12.0% (US) and -15.0% (Europe) in 2005-2020, the decreases mainly occurred in 2010-2014, corresponding to the reported slowed declines in free tropospheric NO_2. Our analysis thus suggests limited impacts of local emission declines on tropospheric O_3 over the US and Europe

https://doi.org/10.5194/acp-2023-47
Preprint. Discussion started: 17 April 2023


Atmospheric Chemistry and Physics Discussions

and advises more efforts to evaluate the possible contributions of natural sources and transport.

1. Introduction

The successful emission regulations employed in the United States (US) and Europe (Crippa et al., 2016; EPA, 2017) have led to dramatic decreases in anthropogenic NO_x emissions (Di et al., 2020; Macdonald et al., 2021; Jiang et al., 2022). As an important air pollutant, tropospheric ozone (O_3) is produced when volatile organic compounds (VOC) are photochemically oxidized in the presence of nitrogen oxides (NO_x). As a major precursor of tropospheric O_3, decreases in surface nitrogen dioxide (NO_2) concentrations, driven by declines in NO_x emissions, have led to marked decreases in surface O_3 concentrations over the US and Europe in recent decades. For example, Chen et al. (2021) found a decrease in surface O_3 concentrations from approximately 60 to 45 ppb over the US in 1990-2019; Seltzer et al. (2020) exhibited a decreasing trend of surface O_3 by approximately 0.8 ppb yr^{-1} over the US in 2000-2015; and Yan et al. (2018) found a decreasing trend of surface O_3 concentrations by approximately 0.32 $\mu g/m^3/y$ over Europe in 1995-2014.

While NO_x emissions are declining, the shift of NO_x sources from power generation to industrial and transportation sectors has led to diminishing effects in NO_x emission controls (Jiang et al., 2022). Furthermore, recent studies have demonstrated a slowdown in tropospheric NO_2 column declines with respect to surface NO_2 concentrations over the US since approximately 2010 (Jiang et al., 2018; Laughner and Cohen, 2019; Qu et al., 2021). Jiang et al. (2022) further indicated a slowdown of declines in tropospheric NO_2 columns with respect to surface NO_2 concentrations over both the US and Europe. Unlike surface O_3, which is strongly affected by local emissions, free tropospheric O_3 is more susceptible to the influences of free tropospheric sources and sinks, long-range transport, and stratospheric intrusion (Jiang et al., 2015; Xue et al., 2021; Trickl et al., 2020). The different trends in surface and free

https://doi.org/10.5194/acp-2023-47
Preprint. Discussion started: 17 April 2023


Atmospheric Chemistry and Physics Discussions

tropospheric NO_2 may thus result in different changes in surface and free tropospheric O_3 over the US and Europe.

A single tracer tagged-O_3 mode of the GEOS-Chem model was developed in the companion paper (Part 1, Zhu et al. (2023)) and was combined with Ozone Monitoring Instrument (OMI) and surface O_3 observations in China in 2015-2020 via a sequential Kalman Filter (KF) assimilation system (Tang et al., 2022; Han et al., 2022). The rapid O_3 assimilation capability with approximately 91-94% reductions in computational costs (Part 1, Zhu et al. (2023)) provides a new opportunity to extend atmospheric O_3 observations and mitigate the influence of uncertainties in physical and chemical processes (Li et al., 2019; Chen et al., 2022) and emission inventories (Zheng et al., 2017; Jiang et al., 2022). As the second part of this work, we assimilate OMI and US Air Quality System (AQS) and European AirBase network O_3 observations in this paper to constrain tropospheric O_3 in the US and Europe in 2005-2020 with a 0.5°×0.625° horizontal resolution. A comparative analysis by assimilating satellite and surface O_3 observations is useful for better characterization of O_3 changes in the surface and free troposphere. Furthermore, this analysis helps evaluate the long-term performance of the GEOS-Chem model in simulating tropospheric O_3 and can provide new insights into tropospheric O_3 changes associated with reported changes in tropospheric NO_2.

We refer the reader to the companion paper (Part 1, Zhu et al. (2023)) for details about the development and performance of the tagged-O_3 mode of the GEOS-Chem model, O_3 observations (OMI, AQS and AirBase) and the tagged-O_3-based assimilation system by assimilating satellite and surface O_3 observations. The total anthropogenic NO_x and VOC emissions in the GEOS-Chem simulations in this work are scaled following Jiang et al. (2022). The total anthropogenic NO_x emissions in the a priori simulations declined by 53% (US) and 50% (Europe) in 2005-2020; the total anthropogenic VOC emissions in the a priori simulations declined by 19% (US) and 33% (Europe) in 2005-2020. The modeled tropospheric NO_2 and

https://doi.org/10.5194/acp-2023-47
Preprint. Discussion started: 17 April 2023

Atmospheric Chemistry and Physics Discussions

VOC concentrations in this work are thus identical to Jiang et al. (2022) in 2005-2018.

2. Results and Discussion

2.1 Surface O_3 by assimilating surface O_3 observations

As shown in Fig. 1, five regions (i.e., Great Lakes (#1), Northeast US (#2), West Coast (#3), Middle US (#4) and Southeast US (#5)) are defined within the US domain, and five regions (i.e., Britain (#1), Central EU (#2), Western EU (#3), Iberian Peninsula (#4) and Apennine Peninsula (#5)) are defined within the European domain based on anthropogenic NO_x emissions in 2015. Regions #1-3 (US) and regions #1-2 (Europe) are defined as highly polluted regions by excluding grids with low and medium anthropogenic NO_x emissions. Tropospheric O_3 changes over these regions will be discussed in this work to investigate the possible regional discrepancies in surface and free tropospheric O_3 changes associated with different local pollution levels.

Fig. 2A-E (US) and Fig. 2A-E (Europe) show the annual and seasonal averages of surface maximum daily 8-hour average (MDA8) O_3 observations from US AQS and European AirBase stations in 2005-2020. Fig. 2K-O (US) and Fig. 2K-O (Europe) further show the annual and seasonal averages of the a posteriori O_3 concentrations by assimilating AQS or AirBase O_3 observations. As shown in Fig. 3 and Fig. 4, the assimilated O_3 concentrations (blue lines) show good agreements with surface O_3 observations (red lines): the mean surface MDA8 O_3 in 2005-2020 are 41.4, 39.5 and 39.5 ppb (US), 40.0, 37.7 and 38.2 ppb (Great Lakes), 38.1, 36.4 and 37.4 ppb (Northeast US), 41.6, 41.2 and 41.0 ppb (West Coast), 42.2, 40.4 and 39.7 ppb (Middle US), 44.4, 40.3 and 39.9 ppb (Southeast US) in the a priori simulations, a posteriori simulations and AQS observations, respectively; the mean surface MDA8 O_3 in 2015-2020 are 35.3, 32.0 and 31.6 ppb (Europe), 29.9, 26.0 and 24.4 ppb (Britain), 30.5, 28.2 and 28.0 ppb (Central EU), 35.9, 32.5 and 32.3 ppb (Western EU), 40.3, 35.2 and 34.2 ppb

https://doi.org/10.5194/acp-2023-47
Preprint. Discussion started: 17 April 2023


Atmospheric Chemistry and Physics Discussions

(Iberian Peninsula), 41.8, 35.3 and 34.0 ppb (Apennine Peninsula) in the a priori simulations, a posteriori simulations and AirBase observations, respectively.

Similar to China, we find overestimated summertime surface O_3 concentrations in the a priori simulations over the US and Europe (Fig. 3 and Fig. 4). However, in contrast to the underestimated O_3 declines in June-July in China (Part 1, Zhu et al. (2023)), the overestimated summertime O_3 over the US and Europe are caused by overestimated increases in surface O_3 in July-August, which have led to surface MDA8 O_3 maximum in July-August in the simulations. In contrast, assimilations suggest that surface O_3 is broadly maximum in April over the US and Europe (Fig. 3 and Fig. 4), although O_3 seasonality varies over different regions. We find good agreements in surface O_3 concentrations between a priori and a posteriori simulations over the US in seasons outside of summer (Fig. 2P-T), in contrast to the large differences between a priori and a posteriori simulations over Europe (Fig. 2 in this work) and China (Part 1, Zhu et al. (2023)). The inaccurate surface O_3 concentrations over three continents reveal possible uncertainties in model simulations, particularly the contributions from natural and anthropogenic processes; for example, the higher temperature and solar radiation can lead to high O_3 concentrations in August, whereas the transport of O_3 and its precursors can lead to high O_3 concentrations in April (Parrish et al., 2013).

Furthermore, our analysis exhibits high surface MDA8 O_3 concentrations over the West Coast (41.2 ppb) in the US. Except for the West Coast, the assimilated surface MDA8 O_3 concentrations are lower over areas with higher anthropogenic NO_x emissions over the US and Europe. For example, 37.7 and 36.4 ppb in the Great Lakes and Northeast US, respectively, in contrast to 40.4 and 40.3 ppb in the Middle US and Southeast US, respectively; and 26.0 and 28.2 ppb in the Britain and Central EU, respectively, in contrast to 32.5, 35.2 and 35.3 ppb in the Western EU, Iberian Peninsula and Apennine Peninsula, respectively. The inverse relationships between surface O_3 concentrations and local anthropogenic NO_x emissions

https://doi.org/10.5194/acp-2023-47
Preprint. Discussion started: 17 April 2023


Atmospheric Chemistry and Physics Discussions

indicate the important impacts of natural sources and meteorological conditions on surface O_3 pollution over the US and Europe. This is the opposite of the higher O_3 concentrations in areas with higher local anthropogenic NO_x emissions in China (Part 1, Zhu et al. (2023)), where surface O_3 pollution is strongly affected by anthropogenic emissions.

2.2 Limited changes in surface O_3 concentrations

Following Jiang et al. (2022), the anthropogenic NO_x and VOC emissions over the US in 2005-2020 declined by 53% (-5.1% yr^{-1}) and 19% (-1.4% yr^{-1}) in our a priori simulations, which is accompanied by slight decreasing trends in surface MDA8 O_3 in the a priori simulations (Table 1.1): -0.29 (spring), -0.45 (summer), -0.07 (autumn) and 0.05 (winter) ppb yr^{-1}; and the relative trends are -0.7 (spring), -0.9 (summer), -0.2 (autumn) and 0.2 (winter) % yr^{-1}. Similarly, the anthropogenic NO_x and VOC emissions over Europe in 2005-2020 declined by 50% (-4.4% yr^{-1}) and 33% (-2.7% yr^{-1}) in our a priori simulations, which is accompanied by slightly increasing trends of surface MDA8 O_3 in the a priori simulations (Table 2.1): -0.07 (spring), -0.07 (summer), 0.07 (autumn) and 0.24 (winter) ppb yr^{-1}; and the relative trends are -0.2 (spring), -0.2 (summer), 0.2 (autumn) and 1.0 (winter) % yr^{-1}. It is surprising to see the limited changes in surface O_3 concentrations in the simulations accompanied by dramatic declines in anthropogenic emissions.

We thus further investigate the changes in surface O_3 by assimilating surface O_3 observations. As shown in Table 1.1 and Fig. 5K-O (US), our assimilations suggest -0.27 (spring), -0.46 (summer), -0.12 (autumn) and 0.11 (winter) ppb yr^{-1} changes in surface MDA8 O_3 over the US in 2005-2020, and the relative changes are -0.6 (spring), -1.0 (summer), -0.3 (autumn) and 0.4 (winter) % yr^{-1}. Similarly, as shown in Table 2.1 and Fig. 5K-O (Europe), our assimilations suggest -0.04 (spring), -0.03 (summer), 0.09 (autumn) and 0.19 (winter) ppb yr^{-1} changes in surface MDA8 O_3 over Europe in 2005-2020, and the relative changes are -0.1 (spring), -0.1 (summer), 0.3 (autumn) and 0.9 (winter) % yr^{-1}. In contrast to the underestimated

https://doi.org/10.5194/acp-2023-47
Preprint. Discussion started: 17 April 2023


Atmospheric Chemistry and Physics Discussions

157 increasing trends in surface O_3 concentrations in the a priori simulations in China (Part 1, Zhu
158 et al. (2023)), we find broadly consistent trends between simulations and assimilations over the
159 US and Europe, which confirms the limited changes in surface O_3 concentrations over the US
160 and Europe.

161 The changes in surface O_3 concentrations have marked regional and seasonal
162 discrepancies. As shown in Tables S1-S5 (see the SI), our assimilations demonstrate stronger
163 increasing trends in surface O_3 concentrations in 2005-2020 in the winter (0.39 ppb yr^{-1} or 1.5%
164 yr^{-1}) over the Great Lakes, in the winter (0.36 ppb yr^{-1} or 1.4% yr^{-1}) over the Northeast US, in
165 the autumn (0.34 ppb yr^{-1} or 0.8% yr^{-1}) and winter (0.29 ppb yr^{-1} or 1.0% yr^{-1}) over the West
166 Coast, as well as decreasing trends in surface O_3 concentrations in 2005-2020 in the summer
167 over the Great Lakes (-0.51 ppb yr^{-1} or -1.0% yr^{-1}), Northeast US (-0.52 ppb yr^{-1} or -1.1% yr^{-1}),
168 Middle US (-0.61 ppb yr^{-1} or -1.3% yr^{-1}) and Southeast US (-0.87 ppb yr^{-1} or -1.9% yr^{-1}). The
169 areas with higher anthropogenic NO_x emissions such as the Great Lakes and Northeast US
170 demonstrate lower surface O_3 concentrations and are accompanied by stronger increasing
171 trends in the winter and weaker decreasing trends in the summer.

172 Tables S6-S10 (see the SI) further show the details of tropospheric O_3 changes in Europe.
173 Our assimilations demonstrate stronger increasing trends in surface O_3 concentrations in 2005-
174 2020 in the winter over Britain (0.28 ppb yr^{-1} or 1.5% yr^{-1}), Central EU (0.26 ppb yr^{-1} or 1.5%
175 yr^{-1}), Western EU (0.25 ppb yr^{-1} or 1.1% yr^{-1}), Iberian Peninsula (0.17 ppb yr^{-1} or 0.6% yr^{-1})
176 and Apennine Peninsula (0.18 ppb yr^{-1} or 0.8% yr^{-1}), as well as decreasing trends in surface O_3
177 concentrations in 2005-2020 in the summer (-0.07 ppb yr^{-1} or -0.2% yr^{-1}) over Britain, in the
178 summer (-0.10 ppb yr^{-1} or -0.2% yr^{-1}) over the Western EU, in the summer (-0.20 ppb yr^{-1} or -
179 0.5% yr^{-1}) over the Iberian Peninsula and in the spring (-0.09 ppb yr^{-1} or -0.2% yr^{-1}) over the
180 Apennine Peninsula. Similar to the US, areas with higher anthropogenic NO_x emissions such
181 as Britain and Central EU demonstrate lower surface O_3 concentrations and are accompanied

https://doi.org/10.5194/acp-2023-47
Preprint. Discussion started: 17 April 2023


Atmospheric Chemistry and Physics Discussions

by stronger increasing trends in the winter and weaker decreasing trends in the summer. It seems that surface O_3 concentrations over the US and Europe are strongly affected by natural sources and meteorological conditions, but their trends are more affected by local anthropogenic emissions.

Furthermore, Zhu et al. (2023) (Part 1) demonstrated a large discrepancy in the trends in assimilated surface O_3 between urban (i.e., areas with air quality stations) and regional backgrounds in China in 2015-2020: 3.0% yr^{-1} (sampled at MEE O_3 observations) and 1.3% yr^{-1} (land average). In contrast, we did not find a comparable discrepancy over the US and Europe: the trends of assimilated surface O_3 are -0.4% yr^{-1} (Table 1.1, sampled at AQS O_3 observations) and -0.4% yr^{-1} (Table 1.2, land average) over the US and -0.2% yr^{-1} (Table 2.1, sampled at AirBase O_3 observations) and 0.0% yr^{-1} (Table 2.2, land average) over Europe. The difference between China and the US/Europe suggests more consistent changes in surface O_3 between urban and regional background areas in the US and Europe. This implies possible larger relative contributions of regional background O_3 to surface O_3 observations in the US and Europe, which could be associated with the limited changes in surface O_3 concentrations in 2005-2020 because regional background O_3 is less sensitive to changes in anthropogenic NO_x and VOC emissions.

2.3 Tropospheric O_3 columns by assimilating OMI O_3 observations

Fig. 6A-E (US) and Fig. 6A-E (Europe) show the annual and seasonal averages of tropospheric OMI O_3 columns in 2005-2020 over the US and Europe, respectively. Fig. 6K-O (US) and Fig. 6K-O (Europe) further show the annual and seasonal averages of the a posteriori tropospheric O_3 columns by assimilating OMI O_3 observations. The assimilated tropospheric O_3 columns show good agreement with OMI O_3 observations: the mean tropospheric O_3 columns over the US in 2005-2020 (Table 1.3) are 35.5 DU in the a priori simulations, and 37.0 and 36.8 DU in the a posteriori simulations and OMI observations, respectively; the mean

https://doi.org/10.5194/acp-2023-47
Preprint. Discussion started: 17 April 2023


Atmospheric Chemistry and Physics Discussions

207 tropospheric O_3 columns over Europe in 2015-2020 (Table 2.3) are 32.8 DU in the a priori
208 simulations, and 35.3 and 36.4 DU in the a posteriori simulations and OMI observations,
209 respectively. Furthermore, as shown in Fig. 7, the trends of tropospheric O_3 columns over the
210 US in 2005-2020 (Table 1.3) are -0.11 DU yr^{-1} in the a priori simulations, and -0.16 and -0.01
211 DU yr^{-1} in the a posteriori simulations and OMI observations, respectively; the trends of
212 tropospheric O_3 columns over Europe in 2015-2020 (Table 2.3) are -0.09 DU yr^{-1} in the a priori
213 simulations, and -0.25 and -0.15 DU yr^{-1} in the a posteriori simulations and OMI observations,
214 respectively.

215 The annual averages of surface MDA8 O_3 in the a priori simulation and assimilations are
216 35.3 and 32.0 ppb with a relative difference of 10% over Europe (Table 2.1); 41.4 and 39.5 ppb
217 with a relative difference of 5% over the US (Table 1.1); and 42.9 and 41.8 ppb with a relative
218 difference of 3% over China (Part 1, Zhu et al. (2023)). In addition, the annual averages of
219 tropospheric O_3 columns in the a priori simulation and assimilations are 32.8 and 35.3 DU with
220 a relative difference of -7% over Europe (Table 2.3); 35.5 and 37.0 DU with a relative
221 difference of -4% over the US (Table 1.3); and 37.1 and 37.9 DU with a relative difference of
222 -2% over China (Part 1, Zhu et al. (2023)). It seems that the GEOS-Chem model has a better
223 performance in regional averages of surface and free tropospheric O_3 concentrations in China
224 and the US than in Europe.

225 The output O_3 profiles from a priori and a posteriori simulations are convolved with OMI
226 averaging kernels in Fig. 6 and Fig. 7. However, the convolution of OMI O_3 averaging kernels
227 on the output O_3 profiles can affect the weights of the derived tropospheric columns to O_3 at
228 different vertical levels and thus may not accurately represent the actual tropospheric O_3
229 columns. Fig. 8 further shows tropospheric O_3 columns from a priori and a posteriori
230 simulations, in which the output O_3 profiles are not convolved with OMI averaging kernels.
231 The assimilated tropospheric O_3 columns are 35.6 and 38.7 DU (US), 36.8 and 40.2 DU (Great

https://doi.org/10.5194/acp-2023-47
Preprint. Discussion started: 17 April 2023


Atmospheric Chemistry and Physics Discussions

232 Lakes), 36.8 and 40.3 DU (Northeast US), 38.1 and 41.9 DU (West Coast), 38.9 and 41.5 DU
233 (Middle US), 43.5 and 45.8 DU (Southeast US) in 2015-2020 by assimilating AQS and OMI
234 O_3 observations, respectively; the assimilated tropospheric O_3 columns are 31.5 and 35.9 DU
235 (Europe), 29.7 and 34.7 DU (Britain), 30.4 and 34.9 DU (Central EU), 31.8 and 36.4 DU
236 (Western EU), 33.6 and 38.1 DU (Iberian Peninsula), 34.0 and 38.2 DU (Apennine Peninsula)
237 in 2015-2020 by assimilating AirBase and OMI O_3 observations, respectively. We find that
238 tropospheric O_3 columns obtained by assimilating surface O_3 observations are lower than those
239 obtained by assimilating OMI O_3 observations. Similar to surface O_3 concentrations,
240 tropospheric O_3 columns are lower over areas with higher anthropogenic NO_x emissions over
241 the US and Europe such as the Great Lakes, Northeast US, Britain and Central EU. This is
242 opposite to the higher tropospheric O_3 columns over areas with higher local anthropogenic NO_x
243 emissions in China (Part 1, Zhu et al. (2023)).

244 In contrast to the surface MDA8 O_3 maximum in April in the observations (Fig. 3 and
245 Fig. 4), the assimilated tropospheric O_3 columns are broadly maximum in July-August over the
246 US and Europe (Fig. 9 and Fig. 10). The free tropospheric O_3 maximum in the summer has
247 been reported in previous studies. For example, Wespes et al. (2018) demonstrated a free
248 tropospheric O_3 maximum in summer over Europe by using Infrared Atmospheric Sounding
249 Interferometer (IASI) observations; Petetin et al. (2016) exhibited a free tropospheric O_3
250 maximum in summer over Europe by using MOZAIC aircraft measurements. We find good
251 agreement in the seasonality of free tropospheric O_3 between simulations and assimilations in
252 contrast to the inaccurate simulation of the seasonality of surface O_3 concentrations in the
253 simulations. More studies are needed in the future to explore the sources of this difference in
254 model performance.

255 Furthermore, Fig. 11 and Fig. 12 demonstrate the O_3 vertical profiles in 2005-2009, 2010-
256 2014 and 2015-2020, respectively. The assimilation of surface O_3 observations leads to

https://doi.org/10.5194/acp-2023-47
Preprint. Discussion started: 17 April 2023


Atmospheric Chemistry and Physics Discussions

257 decreases in O_3 concentrations in the lower troposphere but has small impacts on free
258 tropospheric O_3. In contrast, the assimilation of OMI O_3 observations leads to dramatic
259 enhancements in O_3 concentrations in the middle and upper troposphere without noticeable
260 differences between areas with high and low local anthropogenic NO_x emissions. The
261 enhancement in free tropospheric O_3 by assimilating OMI O_3 observations declined gradually
262 from 2005-2009 to 2015-2020. The adjustment in free tropospheric O_3 by assimilating OMI O_3
263 observations in 2015-2020 is larger but comparable with the adjustment in 2015-2020 in China
264 (Part 1, Zhu et al. (2023)).

265 **2.4 Large decreases in tropospheric O_3 columns**

266 Fig 13 shows the trends in tropospheric O_3 columns in 2005-2020 from a priori
267 simulations and a posteriori simulations by assimilating surface and OMI O_3 observations. The
268 trends of tropospheric O_3 columns in 2005-2020 are -0.07, -0.07 and -0.29 DU yr^{-1} (US), -0.03,
269 -0.03 and -0.29 DU yr^{-1} (Great Lakes), -0.02, -0.02 and -0.31 DU yr^{-1} (Northeast US), -0.02, -
270 0.01 and -0.26 DU yr^{-1} (West Coast), -0.08, -0.07 and -0.24 DU yr^{-1} (Middle US), -0.19, -0.18
271 and -0.28 DU yr^{-1} (Southeast US) in the a priori simulations and a posteriori simulations by
272 assimilating AQS and OMI O_3 observations, respectively; and are 0.03, 0.03 and -0.36 DU yr^{-1}
273 (Europe), 0.00, 0.00 and -0.49 DU yr^{-1} (Britain), 0.04, 0.04 and -0.38 DU yr^{-1} (Central EU),
274 0.02, 0.03 and -0.36 DU yr^{-1} (Western EU), 0.02, 0.02 and -0.30 DU yr^{-1} (Iberian Peninsula), -
275 0.04, 0.04 and -0.26 DU yr^{-1} (Apennine Peninsula) in the a priori simulations and a posteriori
276 simulations by assimilating AirBase and OMI O_3 observations, respectively. Our analysis thus
277 exhibits dramatic underestimations in the decreasing trends in tropospheric O_3 columns in the
278 a priori simulations and assimilations by assimilating surface O_3 observations with respect to
279 OMI-based assimilations.

280 The limited changes in surface O_3 concentrations in the a priori simulations and
281 assimilations by assimilating surface O_3 observations indicate limited influences of declines in

https://doi.org/10.5194/acp-2023-47
Preprint. Discussion started: 17 April 2023


Atmospheric Chemistry and Physics Discussions

local anthropogenic emissions on surface O_3 concentrations in the US and Europe in 2005-2020. We can thus expect insignificant influences of the vertical transport of surface O_3 on the changes in free tropospheric O_3 over the US and Europe in 2005-2020, as illustrated by the flat trends in tropospheric O_3 columns in the a priori simulations and assimilations by assimilating surface O_3 observations (Fig. 9 and Fig. 10), as well as the small impacts of assimilation of surface O_3 observations on free tropospheric O_3 (Fig. 11 and Fig. 12). However, as indicated by Jiang et al. (2022), tropospheric OMI NO_2 columns declined by 36% and 23% in 2005-2018 over the US and Europe, respectively. Are the large decreases in tropospheric O_3 columns by assimilating OMI O_3 observations, i.e., 12.0% (US) and 15.0% (Europe) in 2005-2020, caused by the declines in free tropospheric NO_2?

As indicated by Jiang et al. (2022), tropospheric OMI NO_2 columns declined by -7.0% yr^{-1} (US) and -4.2% yr^{-1} (Europe) in 2005-2010, which was followed by a dramatic slowdown in the decreasing trends, i.e., -1.7% yr^{-1} (US) and -1.2% yr^{-1} (Europe) in 2010-2018. However, as shown in Table 1.4, tropospheric O_3 columns obtained by assimilating OMI O_3 observations declined by -0.3, -2.3 and -0.5% yr^{-1} over the US in 2005-2009, 2010-2014 and 2015-2020, respectively. Similarly, tropospheric O_3 columns obtained by assimilating OMI O_3 observations declined by -1.0, -2.3 and -0.8% yr^{-1} over Europe (Table 2.4) in 2005-2009, 2010-2014 and 2015-2020, respectively. The OMI-based declines in tropospheric O_3 columns over the US and Europe mainly occurred in the period with slowed decreases in free tropospheric NO_2 after 2010; in contrast, the dramatic declines in tropospheric NO_2 columns before 2010 were accompanied by limited changes in free tropospheric O_3. It is thus difficult to conclude that the large decreases in tropospheric O_3 columns over the US and Europe in 2010-2014 are dominated by declines in local anthropogenic NO_x emissions.

We note our OMI-based analysis could be affected by the row anomaly issue. The usage of “row-isolated” data by using across-track positions between 4-11 in this work (see details in

https://doi.org/10.5194/acp-2023-47
Preprint. Discussion started: 17 April 2023


Atmospheric Chemistry and Physics Discussions

the companion paper (Zhu et al. (2023)) is expected to reduce the impacts of row anomaly. Furthermore, as shown by Huang et al. (2017), the row anomaly can lead to discontinuity in the trends in OMI O_3 observations in 2009. However, the large decreases in tropospheric O_3 columns over the US and Europe mainly occurred after 2010. We thus assume the limited influence of row anomaly on our conclusion, although cautious interpretations are suggested in view of the large difference in the trends of tropospheric O_3 columns by assimilating surface and satellite observations.

3. Conclusion

As a companion paper of Zhu et al. (2023) which focuses on tropospheric O_3 change in China in 2015-2020, this paper investigates the changes in surface and free tropospheric O_3 over the US and Europe in 2005-2020 by assimilating OMI, AQS and AirBase O_3 observations. The assimilated O_3 concentrations demonstrate good agreement with O_3 observations: surface O_3 concentrations are 41.4, 39.5 and 39.5 ppb (US) and 35.3, 32.0 and 31.6 ppb (Europe) in the a priori and a posteriori simulations and AQS and AirBase O_3 observations, respectively; and tropospheric O_3 columns are 35.5, 37.0 and 36.8 DU (US) and 32.8, 35.3 and 36.4 DU (Europe) in the a priori and a posteriori simulations (convolved with OMI retrieval averaging kernels) and OMI O_3 observations, respectively. The modeled surface O_3 by GEOS-Chem is overestimated in the summer, which results in a surface O_3 maximum in July-August in the simulations in contrast to April in the observations; in contrast, GEOS-Chem demonstrates good performance in the simulation of seasonality in free tropospheric O_3, which is maximum in July-August. In addition, we find lower surface O_3 concentrations over areas with higher anthropogenic NO_x emissions in the US and Europe. This is the opposite of the higher O_3 concentrations in areas with higher local anthropogenic NO_x emissions in China (Part 1, Zhu et al. (2023)).

Our analysis exhibits a noticeable decrease in surface O_3 concentrations over the US in

https://doi.org/10.5194/acp-2023-47
Preprint. Discussion started: 17 April 2023


Atmospheric Chemistry and Physics Discussions

the summer by 15% in 2005-2020. However, accompanied by approximately 50% reductions in NO_x emissions, changes in surface O_3 concentrations are limited in Europe and other seasons in the US: the annual surface MDA8 O_3 decreased by -6% over the US and increased by 1.5% over Europe in 2005-2020, and the decreases in surface O_3 concentrations are weaker over areas with higher local anthropogenic NO_x emissions. Furthermore, the surface observation-based assimilations suggest insignificant changes in tropospheric O_3 columns: -3.0% (US) and 1.5% (Europe) in 2005-2020. While the OMI-based assimilations exhibit large decreases in tropospheric O_3 columns, i.e., -12.0% (US) and -15.0% (Europe) in 2005-2020, the decreases in tropospheric O_3 columns mainly occurred in 2010-2014, corresponding to reported slowed declines in free tropospheric NO_2 (Jiang et al., 2022). Despite the dramatic declines in tropospheric NO_2, our analysis suggests limited impacts of local emission declines on changes in tropospheric O_3 over the US and Europe in 2005-2020. More efforts are suggested to evaluate the contributions of natural sources and transport to tropospheric O_3 changes, which is critical for making more effective policies to reduce O_3 pollution.

Code and data availability: The AQS and AirBase surface O_3 data can be downloaded from https://www.eea.europa.eu/data-and-maps/data/aqereporting-8 and https://aqs.epa.gov/aqsweb/airdata/download_files.html#Row. The OMI PROFOZ product can be acquired at https://avdc.gsfc.nasa.gov/pub/data/satellite/Aura/OMI/V03/L2/OMPROFOZ/. The GEOS-Chem model (version 12.8.1) can be downloaded from http://wiki.seas.harvard.edu/geos-chem/index.php/GEOS-Chem_12#12.8.1. The KPP module for tagged-O_3 simulations can be downloaded from https://doi.org/10.5281/zenodo.7545944.

https://doi.org/10.5194/acp-2023-47
Preprint. Discussion started: 17 April 2023

Atmospheric Chemistry and Physics Discussions

Competing interests: The contact author has declared that neither they nor their co-authors have any competing interests.

Acknowledgments: We thank United States Environmental Protection Agency and the European Environmental Agency for providing the surface O_3 measurements. The numerical calculations in this paper have been done on the supercomputing system in the Supercomputing Center of University of Science and Technology of China. This work was supported by the Hundred Talents Program of Chinese Academy of Science and National Natural Science Foundation of China (42277082, 41721002).

Table and Figures

Table 1. Averages (with units ppb or DU) and trends (with units ppb yr^{-1} or DU yr^{-1}) of surface and tropospheric column O_3 concentrations in 2005-2020 over the US from observations (AQS and OMI) and a priori and a posteriori (KF) simulations. T1.1): the modeled surface O_3 is sampled at the locations and times of AQS surface O_3 observations; T1.2): the modeled surface O_3 is averaged over the US (land only); T1.3): the output O_3 profiles from the a priori and a posteriori simulations are convolved with OMI O_3 averaging kernels; T1.4): the output O_3 profiles are NOT convolved with OMI O_3 averaging kernels.

Table 2. Averages (with units ppb or DU) and trends (with units ppb yr^{-1} or DU yr^{-1}) of surface and tropospheric column O_3 concentrations in 2005-2020 over Europe from observations (AirBase and OMI) and a priori and a posteriori (KF) simulations. T2.1): the modeled surface O_3 are sampled at the locations and times of AirBase surface O_3 observations; T2.2): the modeled surface O_3 are averaged over Europe (land only); T2.3): the output O_3 profiles from the a priori and a posteriori simulations are convolved with OMI O_3 averaging kernels; T2.4): the output O_3 profiles are NOT convolved with OMI O_3 averaging kernels.

Fig. 1. (a) Anthropogenic NO_x emissions over the US in 2015; (b) Region definitions for Great Lakes (#1), Northeast US (#2), West Coast (#3), Middle US (#4) and Southeast US (#5). Regions #1-3 are defined as highly polluted (HP) regions by excluding grids with low and medium anthropogenic NO_x emissions. (c) Anthropogenic NO_x emissions over Europe in 2015;

https://doi.org/10.5194/acp-2023-47
Preprint. Discussion started: 17 April 2023


Atmospheric Chemistry and Physics Discussions

(d) Region definitions for Britain (#1), Central EU (#2), Western EU (#3), Iberian Peninsula (#4) and Apennine Peninsula (#5). Regions #1 and #2 are defined as highly polluted (HP) regions by excluding grids with low and medium anthropogenic NO_x emissions. The different colors (red, gray and green) represent grids with high (highest 15%), medium (15-50%) and low (lowest 50%) anthropogenic NO_x emissions.

Fig. 2. Surface MDA8 O_3 in 2005-2020 (annual and seasonal averages) from (A-E) AQS or AirBase stations; (F-J) GEOS-Chem a priori simulation; (K-O) GEOS-Chem a posteriori simulation by assimilating AQS or AirBase O_3 observations. (P-T) bias in the a priori simulations calculated by a priori minus a posteriori O_3 concentrations.

Fig. 3. (A-F) Daily averages of surface MDA8 O_3 in 2005-2020 from AQS stations (red) and GEOS-Chem a priori (black) and a posteriori (blue) simulations by assimilating AQS O_3 observations. (G-L) Monthly averages of MDA8 O_3. The dashed lines in panels G-L are annual averages.

Fig. 4. (A-F) Daily averages of surface MDA8 O_3 in 2005-2020 from AirBase stations (red) and GEOS-Chem a priori (black) and a posteriori (blue) simulations by assimilating AirBase O_3 observations. (G-L) Monthly averages of MDA8 O_3. The dashed lines in panels G-L are annual averages.

Fig. 5. Trends of surface MDA8 O_3 in 2005-2020 (annual and seasonal averages) from (A-E) AQS or AirBase stations; (F-J) GEOS-Chem a priori simulation; (K-O) GEOS-Chem a posteriori simulation by assimilating AQS or AirBase O_3 observations.

Fig. 6. Tropospheric O_3 columns in 2005-2020 (annual and seasonal averages) from (A-E) OMI observations; (F-J) GEOS-Chem a priori simulation; (K-O) GEOS-Chem a posteriori simulation by assimilating OMI O_3 observations. (P-T) bias in the a priori simulations calculated by a priori minus a posteriori tropospheric O_3 columns. The output O_3 profiles are convolved with OMI averaging kernels.

Fig. 7. Trends of tropospheric O_3 columns in 2005-2020 (annual and seasonal averages) from (A-E) OMI observations; (F-J) GEOS-Chem a priori simulation; (K-O) GEOS-Chem a

https://doi.org/10.5194/acp-2023-47
Preprint. Discussion started: 17 April 2023


Atmospheric Chemistry and Physics Discussions

posteriori simulation by assimilating OMI O_3 observations. The output O_3 profiles are convolved with OMI averaging kernels.

Fig. 8. Tropospheric O_3 columns in 2005-2020 (annual and seasonal averages) from (A-E) GEOS-Chem a priori simulation; (F-J) assimilations of AQS or AirBase surface O_3 observations; (K-O) assimilations of OMI O_3 observations. (P-T) difference in tropospheric O_3 columns calculated by OMI-based assimilations minus surface observation-based assimilations.

Fig. 9. (A-F) Daily averages of tropospheric O_3 columns in 2005-2020 from GEOS-Chem a priori simulation (black) and a posteriori simulations by assimilating AQS (blue) and OMI (red) O_3 observations. (G-L) Monthly averages of tropospheric O_3 columns. The dashed lines in panels G-L are annual averages.

Fig. 10. (A-F) Daily averages of tropospheric O_3 columns over Europe in 2005-2020 from GEOS-Chem a priori simulation (black) and a posteriori simulations by assimilating AirBase (blue) and OMI (red) O_3 observations. (G-L) Monthly averages of tropospheric O_3 columns. The dashed lines in panels G-L are annual averages.

Fig. 11. Averages of O_3 vertical profiles in 2005-2020 in the US from GEOS-Chem a priori (black) and a posteriori simulations by assimilating AQS (blue) and OMI (red) O_3 observations.

Fig. 12. Averages of O_3 vertical profiles in 2005-2020 in Europe from GEOS-Chem a priori (black) and a posteriori simulations by assimilating AirBase (blue) and OMI (red) O_3 observations.

Fig. 13. Trends of tropospheric O_3 columns in 2005-2020 (annual and seasonal averages) from (A-E) GEOS-Chem a priori simulation; (F-J) assimilations of AQS or AirBase surface O_3 observations; (K-O) assimilations of OMI O_3 observations.

References

https://doi.org/10.5194/acp-2023-47
Preprint. Discussion started: 17 April 2023

Atmospheric Chemistry and Physics Discussions

450 Chen, J., Jiang, Z., Li, R., Liao, C., Miyazaki, K., and Jones, D. B. A.: Large discrepancy
451 between observed and modeled wintertime tropospheric NO_2 variabilities due to COVID-19
452 controls in China, Environ Res Let, 17, 035007, 10.1088/1748-9326/ac4ec0, 2022.
453 Chen, X., Jiang, Z., Shen, Y., Li, R., Fu, Y., Liu, J., Han, H., Liao, H., Cheng, X., Jones, D. B.
454 A., Worden, H., and Abad, G. G.: Chinese Regulations Are Working—Why Is Surface Ozone
455 Over Industrialized Areas Still High? Applying Lessons From Northeast US Air Quality
456 Evolution, Geophys Res Lett, 48, e2021GL092816, 10.1029/2021gl092816, 2021.
457 Crippa, M., Janssens-Maenhout, G., Dentener, F., Guizzardi, D., Sindelarova, K., Muntean,
458 M., Van Dingenen, R., and Granier, C.: Forty years of improvements in European air quality:
459 regional policy-industry interactions with global impacts, Atmos Chem Phys, 16, 3825-3841,
460 10.5194/acp-16-3825-2016, 2016.
461 Di, Q., Amini, H., Shi, L., Kloog, I., Silvern, R., Kelly, J., Sabath, M. B., Choirat, C., Koutrakis,
462 P., Lyapustin, A., Wang, Y., Mickley, L. J., and Schwartz, J.: Assessing NO2 Concentration
463 and Model Uncertainty with High Spatiotemporal Resolution across the Contiguous United
464 States Using Ensemble Model Averaging, Environ Sci Technol, 54, 1372-1384,
465 10.1021/acs.est.9b03358, 2020.
466 United States Environmental Protection Agency: Overview of the Clean Air Act and Air
467 Pollution: https://www.epa.gov/clean-air-act-overview, 2017.
468 Han, W., He, T.-L., Tang, Z., Wang, M., Jones, D., and Jiang, Z.: A comparative analysis for
469 a deep learning model (hyDL-CO v1.0) and Kalman filter to predict CO concentrations in
470 China, Geosci Model Dev, 15, 4225-4237, 10.5194/gmd-15-4225-2022, 2022.
471 Huang, G., Liu, X., Chance, K., Yang, K., Bhartia, P. K., Cai, Z., Allaart, M., Ancellet, G.,
472 Calpini, B., Coetzee, G. J. R., Cuevas-Agulló, E., Cupeiro, M., De Backer, H., Dubey, M. K.,
473 Fuelberg, H. E., Fujiwara, M., Godin-Beekmann, S., Hall, T. J., Johnson, B., Joseph, E., Kivi,
474 R., Kois, B., Komala, N., König-Langlo, G., Laneve, G., Leblanc, T., Marchand, M.,
475 Minschwaner, K. R., Morris, G., Newchurch, M. J., Ogino, S.-Y., Ohkawara, N., Piters, A. J.
476 M., Posny, F., Querel, R., Scheele, R., Schmidlin, F. J., Schnell, R. C., Schrems, O., Selkirk,
477 H., Shiotani, M., Skrivánková, P., Stübi, R., Taha, G., Tarasick, D. W., Thompson, A. M.,
478 Thouret, V., Tully, M. B., Van Malderen, R., Vömel, H., von der Gathen, P., Witte, J. C., and
479 Yela, M.: Validation of 10-year SAO OMI Ozone Profile (PROFOZ) product using
480 ozonesonde observations, Atmos Meas Tech, 10, 2455-2475, 10.5194/amt-10-2455-2017,
481 2017.
482 Jiang, Z., Worden, J. R., Jones, D. B. A., Lin, J. T., Verstraeten, W. W., and Henze, D. K.:
483 Constraints on Asian ozone using Aura TES, OMI and Terra MOPITT, Atmos Chem Phys,
484 15, 99-112, 10.5194/acp-15-99-2015, 2015.
485 Jiang, Z., McDonald, B. C., Worden, H., Worden, J. R., Miyazaki, K., Qu, Z., Henze, D. K.,
486 Jones, D. B. A., Arellano, A. F., Fischer, E. V., Zhu, L., and Boersma, K. F.: Unexpected
487 slowdown of US pollutant emission reduction in the past decade, Proc Natl Acad Sci USA,
488 115, 5099-5104, 10.1073/pnas.1801191115, 2018.
489 Jiang, Z., Zhu, R., Miyazaki, K., McDonald, B. C., Klimont, Z., Zheng, B., Boersma, K. F.,
490 Zhang, Q., Worden, H., Worden, J. R., Henze, D. K., Jones, D. B. A., Denier van der Gon,
491 H. A. C., and Eskes, H.: Decadal Variabilities in Tropospheric Nitrogen Oxides Over United

https://doi.org/10.5194/acp-2023-47
Preprint. Discussion started: 17 April 2023

States, Europe, and China, J Geophys Res-Atmos, 127, e2021JD035872, 10.1029/2021jd035872, 2022.

Laughner, J. L., and Cohen, R. C.: Direct observation of changing NO_x lifetime in North American cities, Science, 366, 723-727, 10.1126/science.aax6832, 2019.

Li, K., Jacob, D. J., Liao, H., Zhu, J., Shah, V., Shen, L., Bates, K. H., Zhang, Q., and Zhai, S.: A two-pollutant strategy for improving ozone and particulate air quality in China, Nat Geosci, 12, 906-910, 10.1038/s41561-019-0464-x, 2019.

Macdonald, E., Otero, N., and Butler, T.: A comparison of long-term trends in observations and emission inventories of NO_x, Atmos Chem Phys, 21, 4007-4023, 10.5194/acp-21-4007-2021, 2021.

Parrish, D. D., Law, K. S., Staehelin, J., Derwent, R., Cooper, O. R., Tanimoto, H., Volz-Thomas, A., Gilge, S., Scheel, H. E., Steinbacher, M., and Chan, E.: Lower tropospheric ozone at northern midlatitudes: Changing seasonal cycle, Geophys Res Lett, 40, 1631-1636, 10.1002/grl.50303, 2013.

Petetin, H., Thouret, V., Fontaine, A., Sauvage, B., Athier, G., Blot, R., Boulanger, D., Cousin, J.-M., and Nédélec, P.: Characterising tropospheric O₃ and CO around Frankfurt over the period 1994–2012 based on MOZAIC–IAGOS aircraft measurements, Atmos Chem Phys, 16, 15147-15163, 10.5194/acp-16-15147-2016, 2016.

Qu, Z., Jacob, D. J., Silvern, R. F., Shah, V., Campbell, P. C., Valin, L. C., and Murray, L. T.: US COVID‐19 Shutdown Demonstrates Importance of Background NO_2 in Inferring NO_x Emissions From Satellite NO_2 Observations, Geophys Res Lett, 48, 10.1029/2021gl092783, 2021.

Seltzer, K. M., Shindell, D. T., Kasibhatla, P., and Malley, C. S.: Magnitude, trends, and impacts of ambient long-term ozone exposure in the United States from 2000 to 2015, Atmos Chem Phys, 20, 1757-1775, 10.5194/acp-20-1757-2020, 2020.

Tang, Z., Chen, J., and Jiang, Z.: Discrepancy in assimilated atmospheric CO over East Asia in 2015–2020 by assimilating satellite and surface CO measurements, Atmos Chem Phys, 22, 7815-7826, 10.5194/acp-22-7815-2022, 2022.

Trickl, T., Vogelmann, H., Ries, L., and Sprenger, M.: Very high stratospheric influence observed in the free troposphere over the northern Alps – just a local phenomenon?, Atmos Chem Phys, 20, 243-266, 10.5194/acp-20-243-2020, 2020.

Wespes, C., Hurtmans, D., Clerbaux, C., Boynard, A., and Coheur, P.-F.: Decrease in tropospheric O_3 levels in the Northern Hemisphere observed by IASI, Atmos Chem Phys, 18, 6867-6885, 10.5194/acp-18-6867-2018, 2018.

Xue, L., Ding, A., Cooper, O., Huang, X., Wang, W., Zhou, D., Wu, Z., McClure-Begley, A., Petropavlovskikh, I., Andreae, M. O., and Fu, C.: ENSO and Southeast Asian biomass burning modulate subtropical trans-Pacific ozone transport, Natl Sci Rev, 8, nwaa132, 10.1093/nsr/nwaa132, 2021.

Yan, Y., Pozzer, A., Ojha, N., Lin, J., and Lelieveld, J.: Analysis of European ozone trends in the period 1995–2014, Atmos Chem Phys, 18, 5589-5605, 10.5194/acp-18-5589-2018, 2018.

https://doi.org/10.5194/acp-2023-47
Preprint. Discussion started: 17 April 2023

Atmospheric Chemistry and Physics Discussions

532 Zheng, B., Zhang, Q., Tong, D., Chen, C., Hong, C., Li, M., Geng, G., Lei, Y., Huo, H., and
533 He, K.: Resolution dependence of uncertainties in gridded emission inventories: a case study
534 in Hebei, China, Atmos Chem Phys, 17, 921-933, 10.5194/acp-17-921-2017, 2017.
535 Zhu, R., Tang, Z., Chen, X., Jiang, Z., and Liu, X.: Rapid assimilations of O_3 observations –
536 Part 1: methodology and tropospheric O_3 changes in China in 2015-2020, submitted to Atmos
537 Chem Phys, 2023.

https://doi.org/10.5194/acp-2023-47
Preprint. Discussion started: 17 April 2023

Atmospheric Chemistry and Physics Discussions

United States			Annual		Spring		Summer		Autumn		Winter	
			Mean	Trend	Mean	Trend	Mean	Trend	Mean	Trend	Mean	Trend
T1.1 surface (sampled)	2005-2020	AQS	39.5	-0.18	45.4	-0.26	45.2	-0.49	36.2	-0.18	31.5	0.14
		a priori	41.4	-0.18	44.2	-0.29	51.2	-0.45	39.2	-0.07	30.9	0.05
		KF-AQS	39.5	-0.17	44.8	-0.27	46.0	-0.46	36.3	-0.12	31.1	0.11
T1.2 surface	2005-2020	a priori	40.3	-0.17	43.3	-0.28	49.1	-0.36	38.1	-0.10	30.8	0.04
		KF-AQS	39.2	-0.15	43.5	-0.25	46.1	-0.34	36.4	-0.12	31.0	0.07
T1.3 trop. column (convolved)	2005-2020	OMI	36.8	-0.01	38.5	0.00	42.1	0.11	34.3	-0.14	32.0	-0.03
		a priori	35.5	-0.11	36.9	-0.14	41.9	-0.15	33.5	-0.08	29.8	-0.06
		KF-OMI	37.0	-0.16	39.4	-0.21	43.3	-0.02	34.6	-0.18	30.7	-0.21
T1.4 trop. Column	2005-2020	a priori	35.9	-0.07	37.4	-0.16	41.2	-0.17	33.4	-0.01	31.6	0.02
		KF-AQS	35.6	-0.07	37.4	-0.15	40.4	-0.16	33.1	-0.01	31.6	0.02
		KF-OMI	38.7	-0.29	41.9	-0.42	43.9	-0.11	35.6	-0.26	33.3	-0.41
	2005-2009	KF-AQS	35.7	-0.25	37.7	-0.45	40.7	-0.97	32.9	-0.12	31.5	-0.13
		KF-OMI	40.1	-0.13	43.5	-0.21	43.5	-0.70	37.1	-0.18	36.5	-0.35
	2010-2014	KF-AQS	36.1	-0.51	38.3	-0.78	41.3	-1.31	33.3	-0.17	31.5	-0.30
		KF-OMI	39.1	-0.89	43.3	-1.20	45.1	-1.37	35.4	-0.41	31.9	-0.67
	2015-2020	KF-AQS	35.1	0.03	36.5	-0.05	39.6	0.15	32.9	0.04	31.8	0.09
		KF-OMI	37.1	-0.18	39.5	-0.43	43.2	-0.02	34.4	-0.21	31.8	-0.03

Table. 1. Averages (with units ppb or DU) and trends (with units ppb yr^{-1} or DU yr^{-1}) of surface and tropospheric column O_3 concentrations in 2005-2020 over the US from observations (AQS and OMI) and a priori and a posteriori (KF) simulations. T1.1): the modeled surface O_3 is sampled at the locations and times of AQS surface O_3 observations; T1.2): the modeled surface O_3 is averaged over the US (land only); T1.3): the output O_3 profiles from the a priori and a posteriori simulations are convolved with OMI O_3 averaging kernels; T1.4): the output O_3 profiles are NOT convolved with OMI O_3 averaging kernels.

https://doi.org/10.5194/acp-2023-47
Preprint. Discussion started: 17 April 2023

Atmospheric Chemistry and Physics Discussions

Europe			Annual		Spring		Summer		Autumn		Winter	
			Mean	Trend	Mean	Trend	Mean	Trend	Mean	Trend	Mean	Trend
T2.1 surface (sampled)	2005-2020	AirBase	31.6	0.08	38.5	-0.02	40.7	0.01	25.7	0.14	21.4	0.22
		a priori	35.3	0.04	40.3	-0.07	46.6	-0.07	31.5	0.07	22.9	0.24
		KF-AirBase	32.0	0.05	38.5	-0.04	41.3	-0.03	26.6	0.09	21.7	0.19
T2.2 surface	2005-2020	a priori	35.5	0.01	40.3	-0.10	46.0	-0.09	31.8	0.04	23.9	0.21
		KF-AirBase	32.5	0.01	38.5	-0.08	41.1	-0.08	27.7	0.04	22.8	0.17
T2.3 trop. column (convolved)	2005-2020	OMI	36.4	-0.15	37.6	-0.33	41.0	-0.09	34.5	-0.12	32.5	-0.09
		a priori	32.8	-0.09	33.6	-0.18	37.3	-0.14	31.3	-0.03	29.0	-0.02
		KF-OMI	35.3	-0.25	37.0	-0.40	40.5	-0.16	33.1	-0.22	30.4	-0.23
T2.4 trop. Column	2005-2020	a priori	32.1	0.03	33.7	-0.03	37.2	0.06	29.5	0.01	27.9	0.06
		KF-AirBase	31.5	0.03	33.3	-0.03	36.2	0.06	28.8	0.01	27.7	0.06
		KF-OMI	35.9	-0.36	39.5	-0.48	41.4	0.02	32.1	-0.38	30.4	-0.58
	2005-2009	KF-AirBase	31.2	-0.24	33.1	-0.17	35.8	-0.39	28.6	-0.40	27.3	-0.22
		KF-OMI	38.1	-0.38	41.6	-0.35	40.9	-0.06	34.6	-0.76	34.9	-1.06
	2010-2014	KF-AirBase	31.4	-0.24	33.6	-0.58	35.8	-0.33	28.7	-0.02	27.4	-0.16
		KF-OMI	35.7	-0.82	40.6	-1.30	41.6	-0.54	31.5	-0.40	28.3	-0.69
	2015-2020	KF-AirBase	31.7	0.03	33.1	-0.03	36.8	0.00	28.9	0.09	28.2	-0.02
		KF-OMI	34.3	-0.26	36.9	-0.58	41.6	-0.28	30.5	-0.19	28.5	-0.11

Table. 2. Averages (with units ppb or DU) and trends (with units ppb yr^{-1} or DU yr^{-1}) of surface and tropospheric column O_3 concentrations in 2005-2020 over Europe from observations (AirBase and OMI) and a priori and a posteriori (KF) simulations. T2.1): the modeled surface O_3 are sampled at the locations and times of AirBase surface O_3 observations; T2.2): the modeled surface O_3 are averaged over Europe (land only); T2.3): the output O_3 profiles from the a priori and a posteriori simulations are convolved with OMI O_3 averaging kernels; T2.4): the output O_3 profiles are NOT convolved with OMI O_3 averaging kernels.

https://doi.org/10.5194/acp-2023-47
Preprint. Discussion started: 17 April 2023

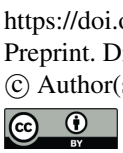

Atmospheric Chemistry and Physics Discussions

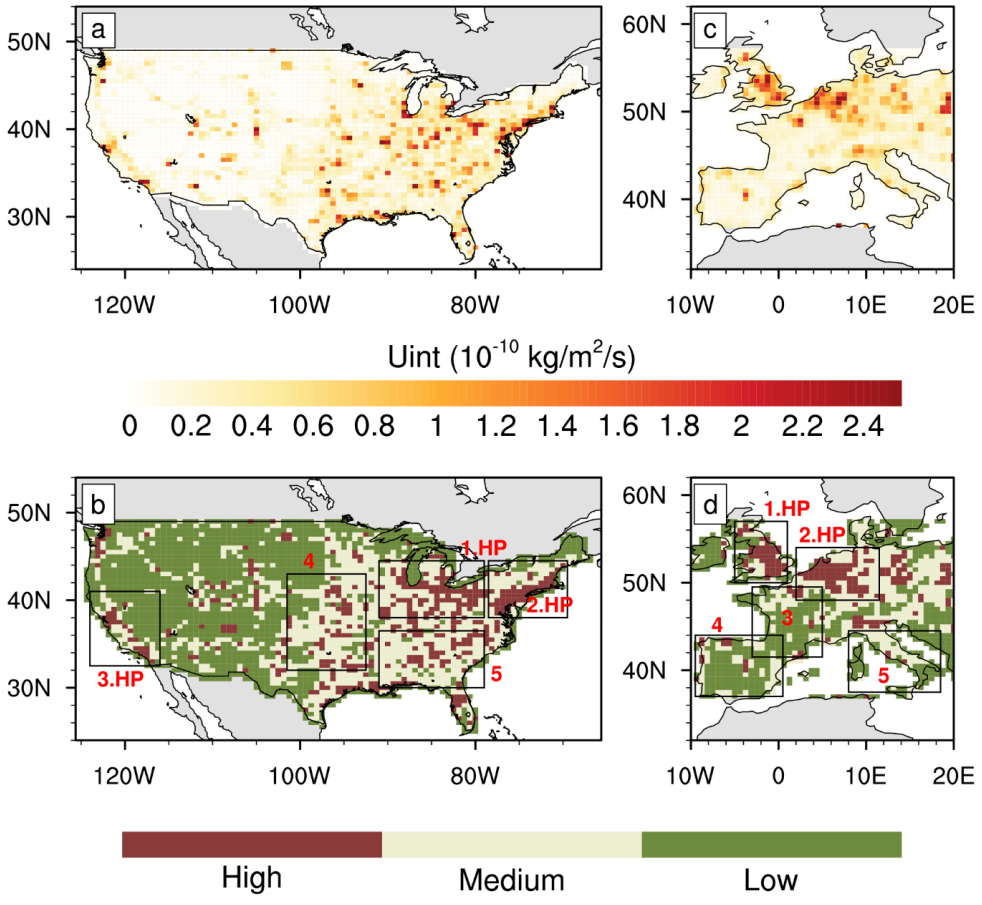

Fig. 1. (a) Anthropogenic NO_x emissions over the US in 2015; (b) Region definitions for Great Lakes (#1), Northeast US (#2), West Coast (#3), Middle US (#4) and Southeast US (#5). Regions #1-3 are defined as highly polluted (HP) regions by excluding grids with low and medium anthropogenic NO_x emissions. (c) Anthropogenic NO_x emissions over Europe in 2015; (d) Region definitions for Britain (#1), Central EU (#2), Western EU (#3), Iberian Peninsula (#4) and Apennine Peninsula (#5). Regions #1 and #2 are defined as highly polluted (HP) regions by excluding grids with low and medium anthropogenic NO_x emissions. The different colors (red, gray and green) represent grids with high (highest 15%), medium (15-50%) and low (lowest 50%) anthropogenic NO_x emissions.

https://doi.org/10.5194/acp-2023-47
Preprint. Discussion started: 17 April 2023

Atmospheric Chemistry and Physics Discussions

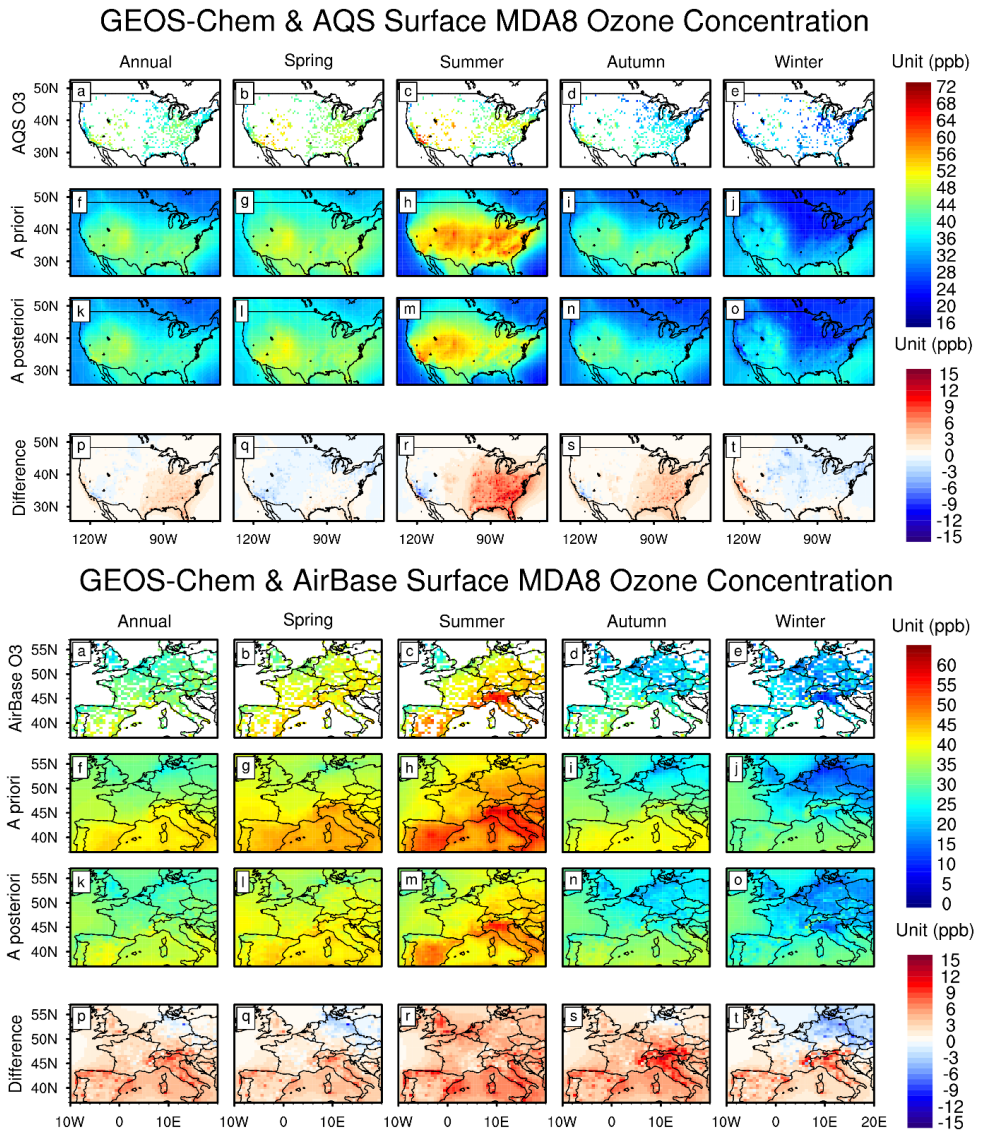

Fig. 2. Surface MDA8 O_3 in 2005-2020 (annual and seasonal averages) from (A-E) AQS or AirBase stations; (F-J) GEOS-Chem a priori simulation; (K-O) GEOS-Chem a posteriori simulation by assimilating AQS or AirBase O_3 observations. (P-T) bias in the a priori simulations calculated by a priori minus a posteriori O_3 concentrations.

https://doi.org/10.5194/acp-2023-47
Preprint. Discussion started: 17 April 2023

Atmospheric Chemistry and Physics Discussions

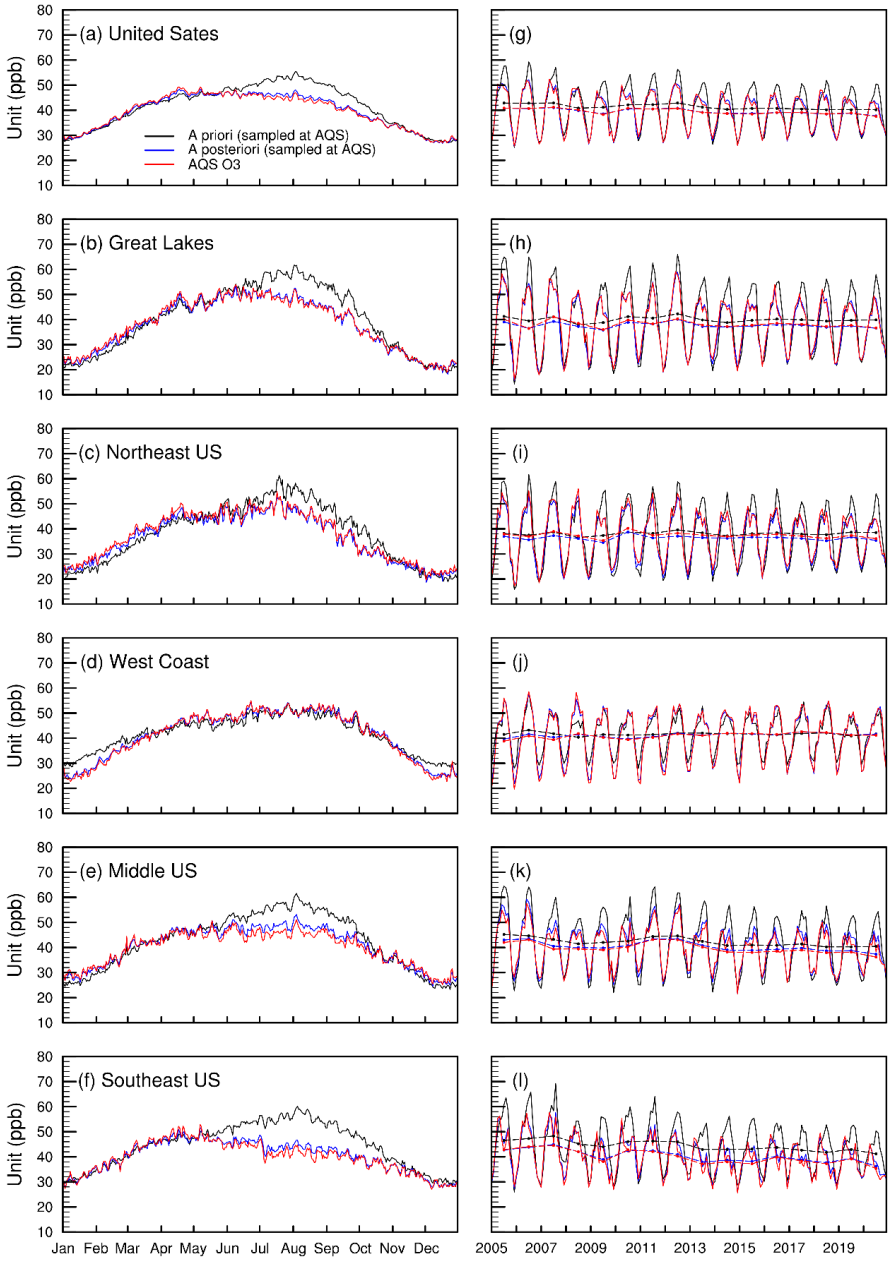

Fig. 3. (A-F) Daily averages of surface MDA8 O_3 in 2005-2020 from AQS stations (red) and GEOS-Chem a priori (black) and a posteriori (blue) simulations by assimilating AQS O_3 observations. (G-L) Monthly averages of MDA8 O_3. The dashed lines in panels G-L are annual averages.

https://doi.org/10.5194/acp-2023-47
Preprint. Discussion started: 17 April 2023

Atmospheric Chemistry and Physics Discussions

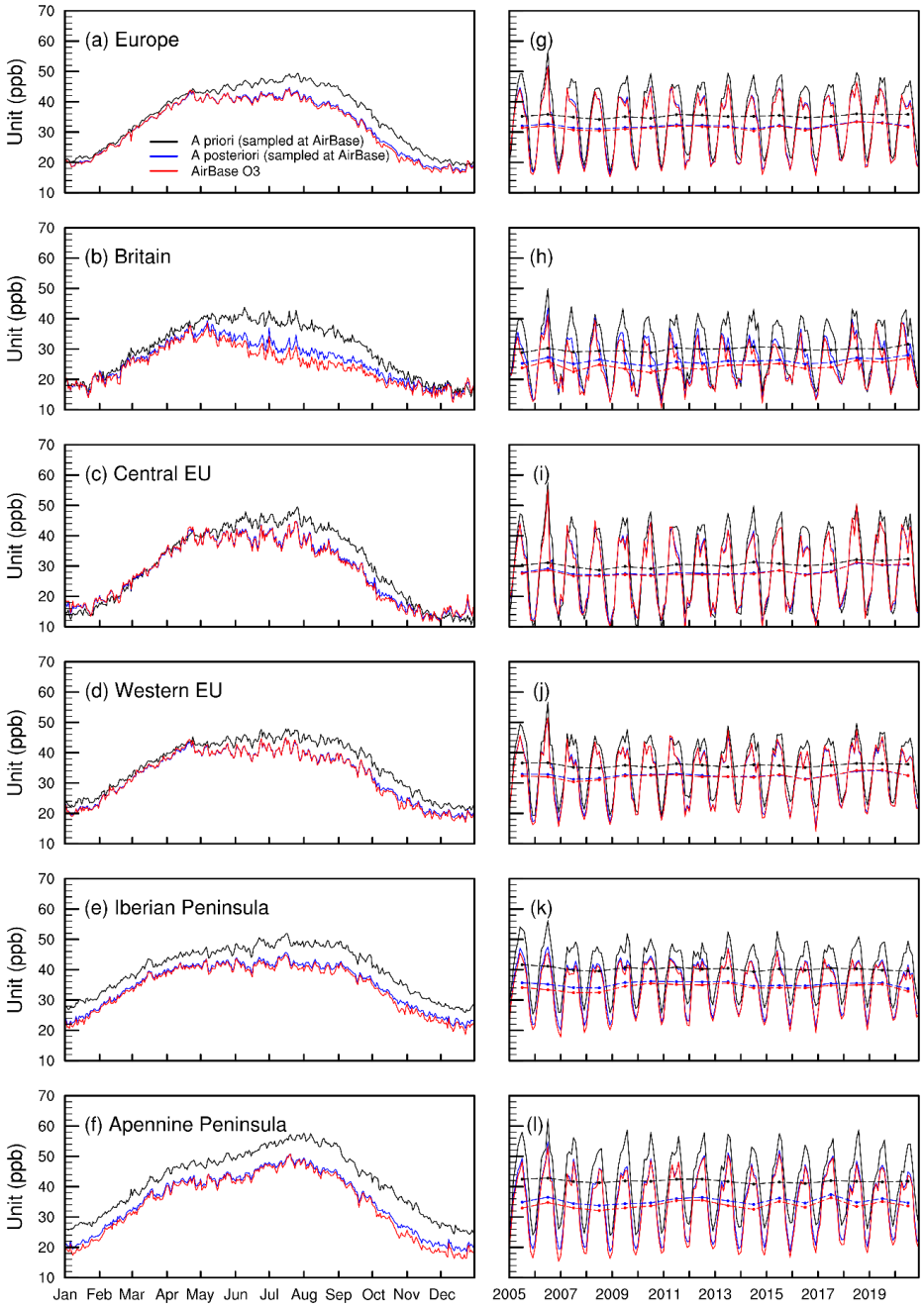

Fig. 4. (A-F) Daily averages of surface MDA8 O_3 in 2005-2020 from AirBase stations (red) and GEOS-Chem a priori (black) and a posteriori (blue) simulations by assimilating AirBase O_3 observations. (G-L) Monthly averages of MDA8 O_3. The dashed lines in panels G-L are annual averages.

https://doi.org/10.5194/acp-2023-47
Preprint. Discussion started: 17 April 2023

Atmospheric Chemistry and Physics Discussions

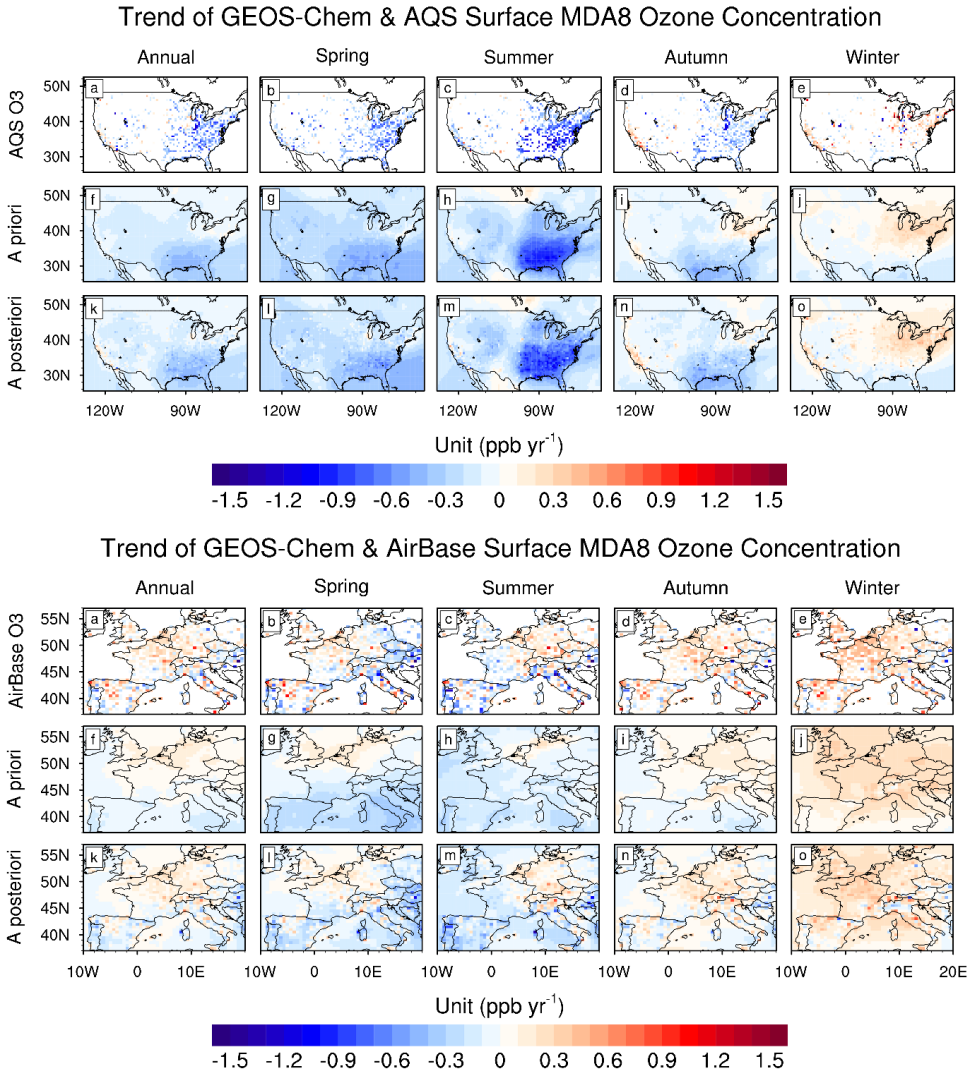

Fig. 5. Trends of surface MDA8 O_3 in 2005-2020 (annual and seasonal averages) from (A-E) AQS or AirBase stations; (F-J) GEOS-Chem a priori simulation; (K-O) GEOS-Chem a posteriori simulation by assimilating AQS or AirBase O_3 observations.

https://doi.org/10.5194/acp-2023-47
Preprint. Discussion started: 17 April 2023

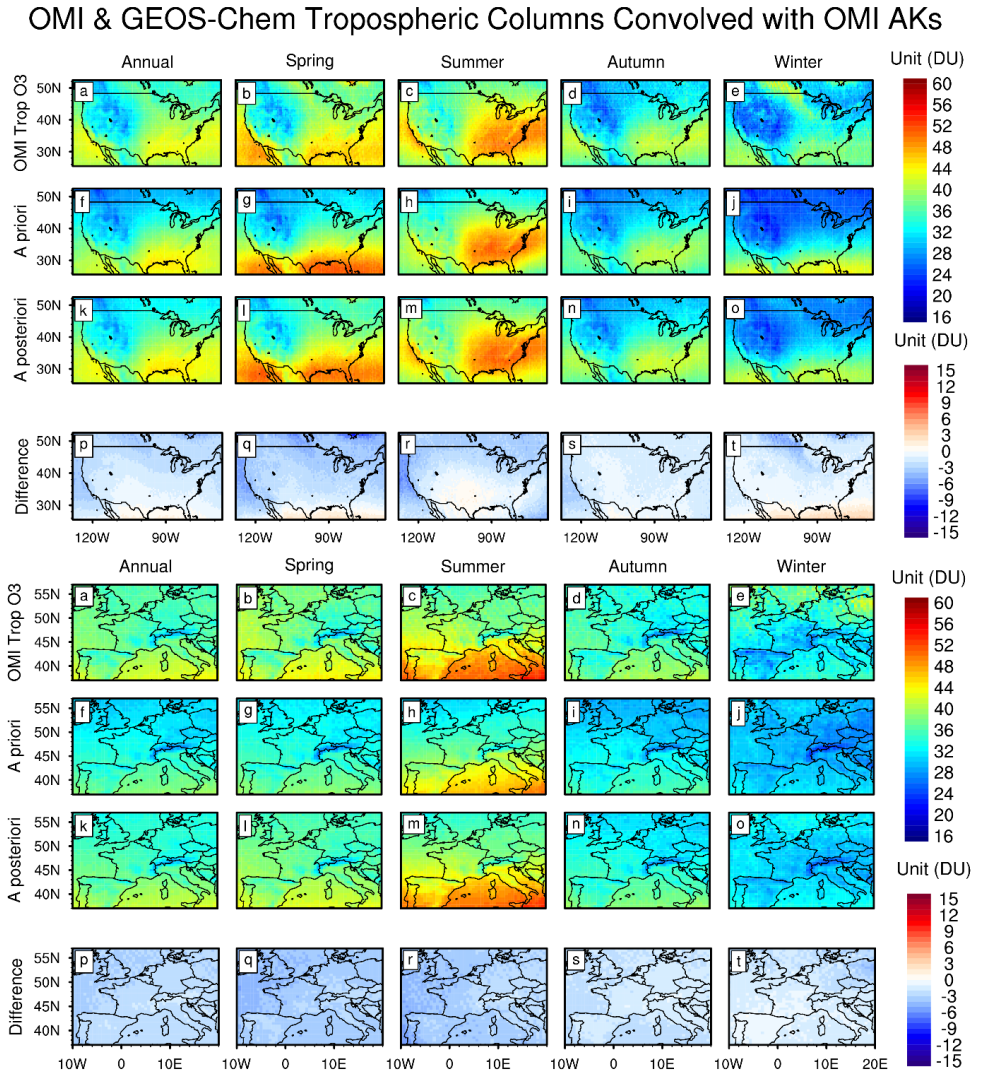

Fig. 6. Tropospheric O_3 columns in 2005-2020 (annual and seasonal averages) from (A-E) OMI observations; (F-J) GEOS-Chem a priori simulation; (K-O) GEOS-Chem a posteriori simulation by assimilating OMI O_3 observations. (P-T) bias in the a priori simulations calculated by a priori minus a posteriori tropospheric O_3 columns. The output O_3 profiles are convolved with OMI averaging kernels.

https://doi.org/10.5194/acp-2023-47
Preprint. Discussion started: 17 April 2023

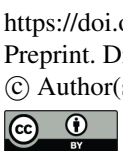

Atmospheric Chemistry and Physics Discussions

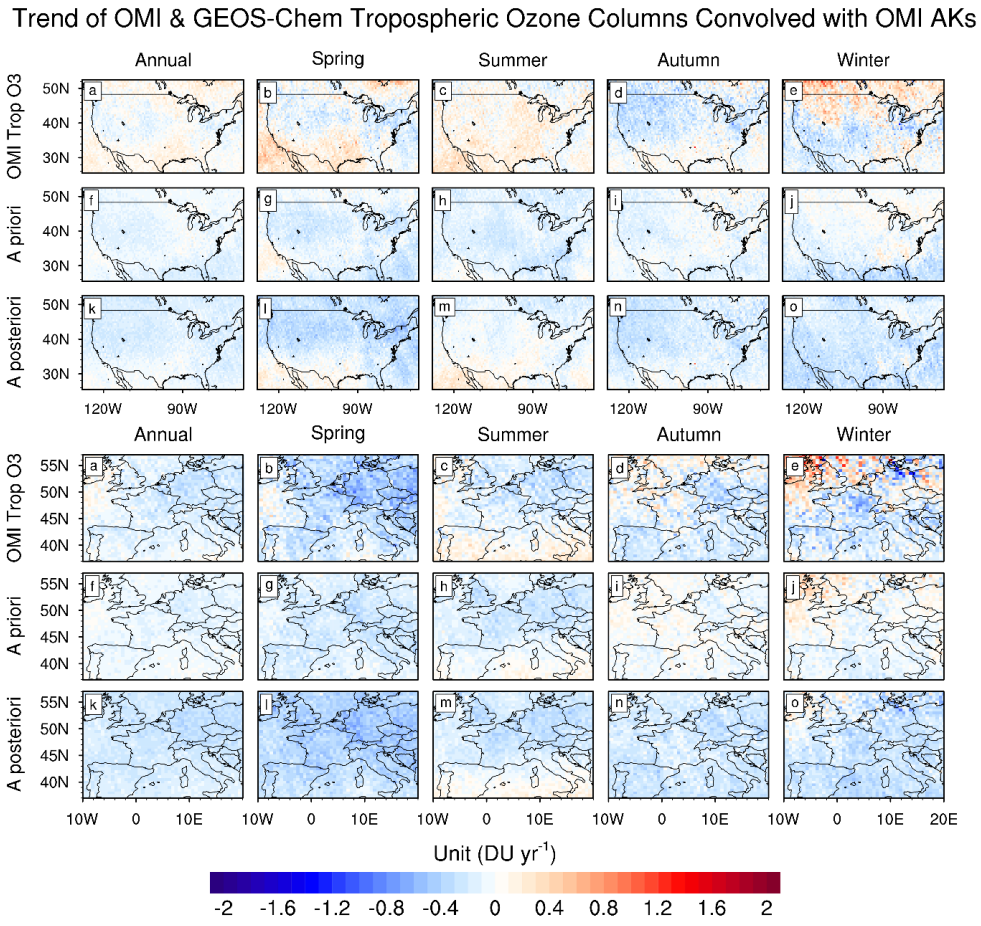

Fig. 7. Trends of tropospheric O_3 columns in 2005-2020 (annual and seasonal averages) from (A-E) OMI observations; (F-J) GEOS-Chem a priori simulation; (K-O) GEOS-Chem a posteriori simulation by assimilating OMI O_3 observations. The output O_3 profiles are convolved with OMI averaging kernels.

https://doi.org/10.5194/acp-2023-47
Preprint. Discussion started: 17 April 2023

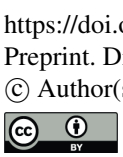

Atmospheric Chemistry and Physics Discussions

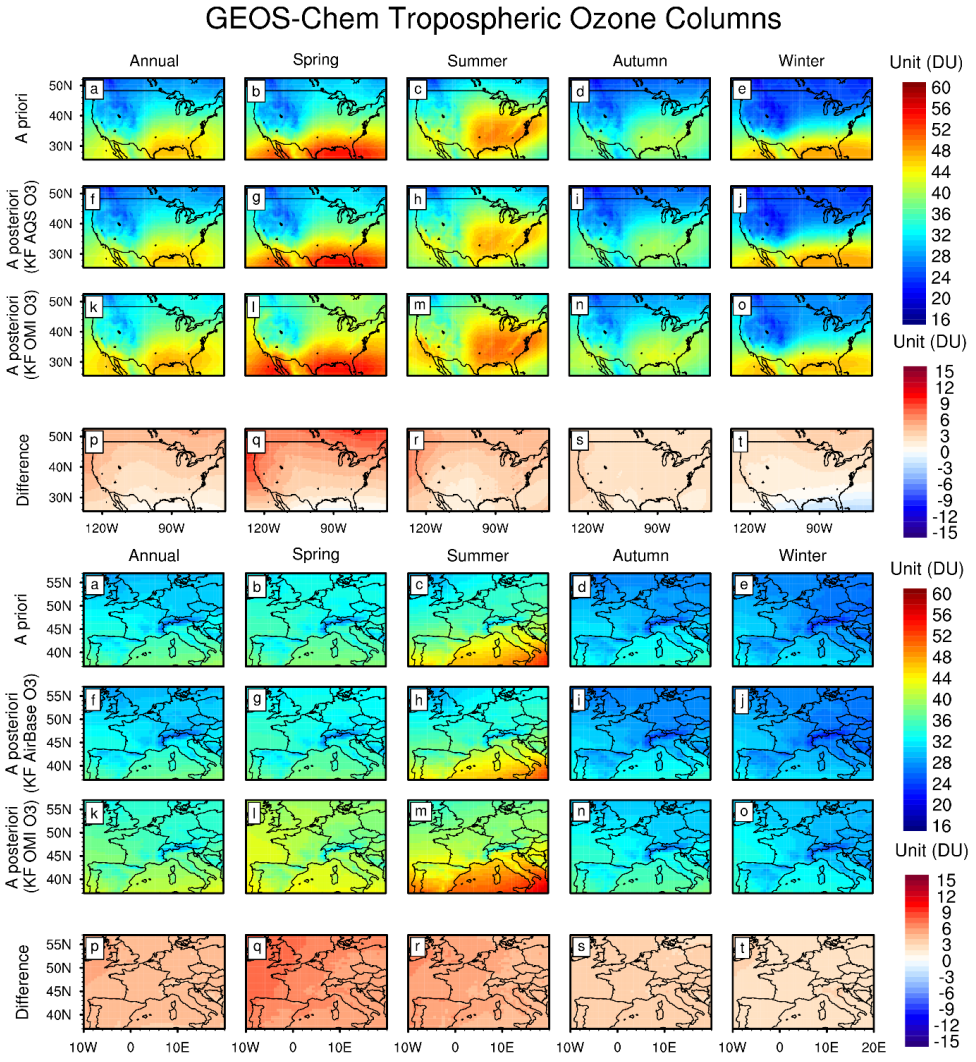

Fig. 8. Tropospheric O_3 columns in 2005-2020 (annual and seasonal averages) from (A-E) GEOS-Chem a priori simulation; (F-J) assimilations of AQS or AirBase surface O_3 observations; (K-O) assimilations of OMI O_3 observations. (P-T) difference in tropospheric O_3 columns calculated by OMI-based assimilations minus surface observation-based assimilations.

https://doi.org/10.5194/acp-2023-47
Preprint. Discussion started: 17 April 2023

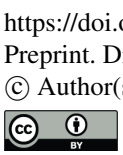

Atmospheric Chemistry and Physics Discussions

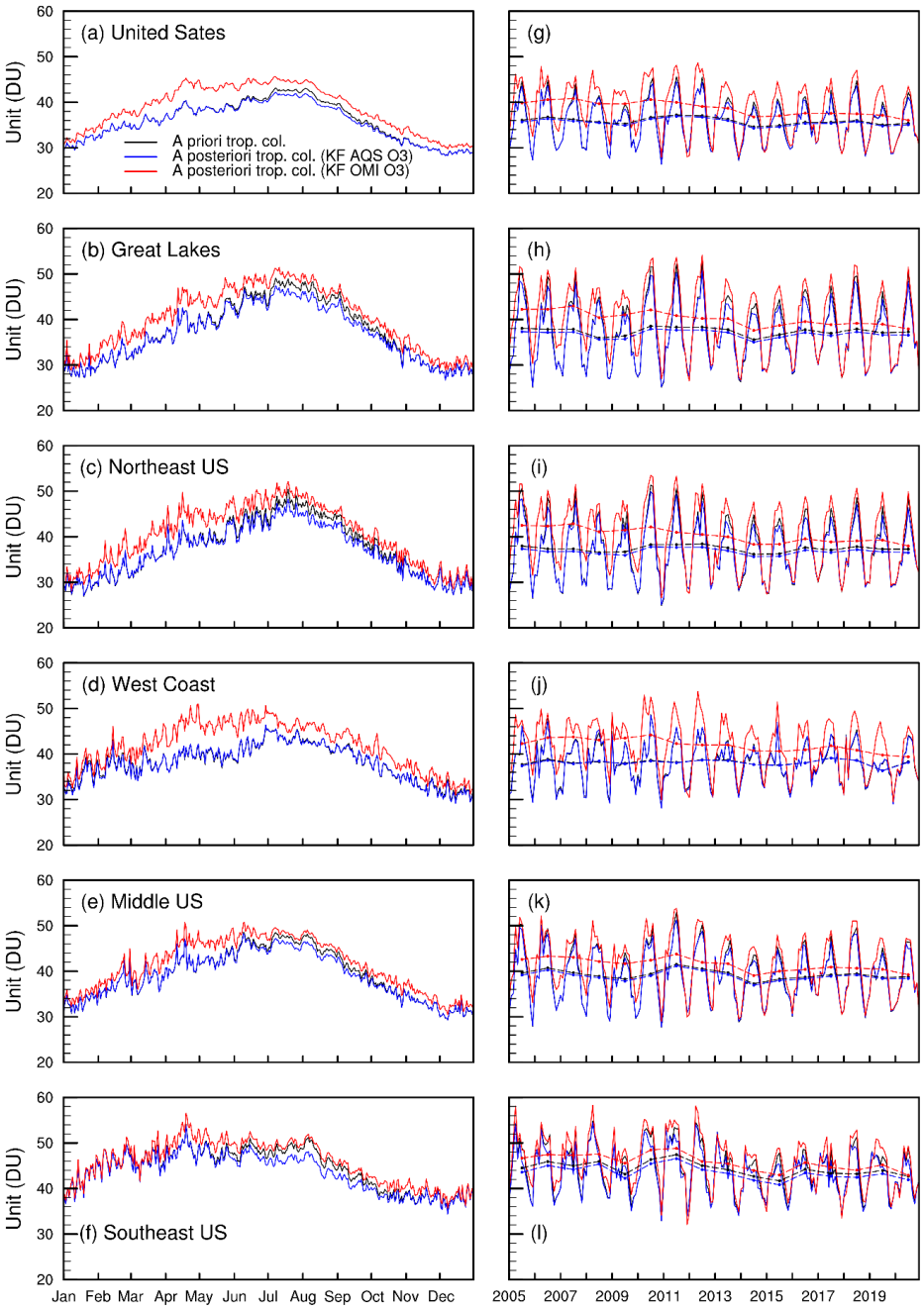

Fig. 9. (A-F) Daily averages of tropospheric O_3 columns in 2005-2020 from GEOS-Chem a priori simulation (black) and a posteriori simulations by assimilating AQS (blue) and OMI (red) O_3 observations. (G-L) Monthly averages of tropospheric O_3 columns. The dashed lines in panels G-L are annual averages.

https://doi.org/10.5194/acp-2023-47
Preprint. Discussion started: 17 April 2023

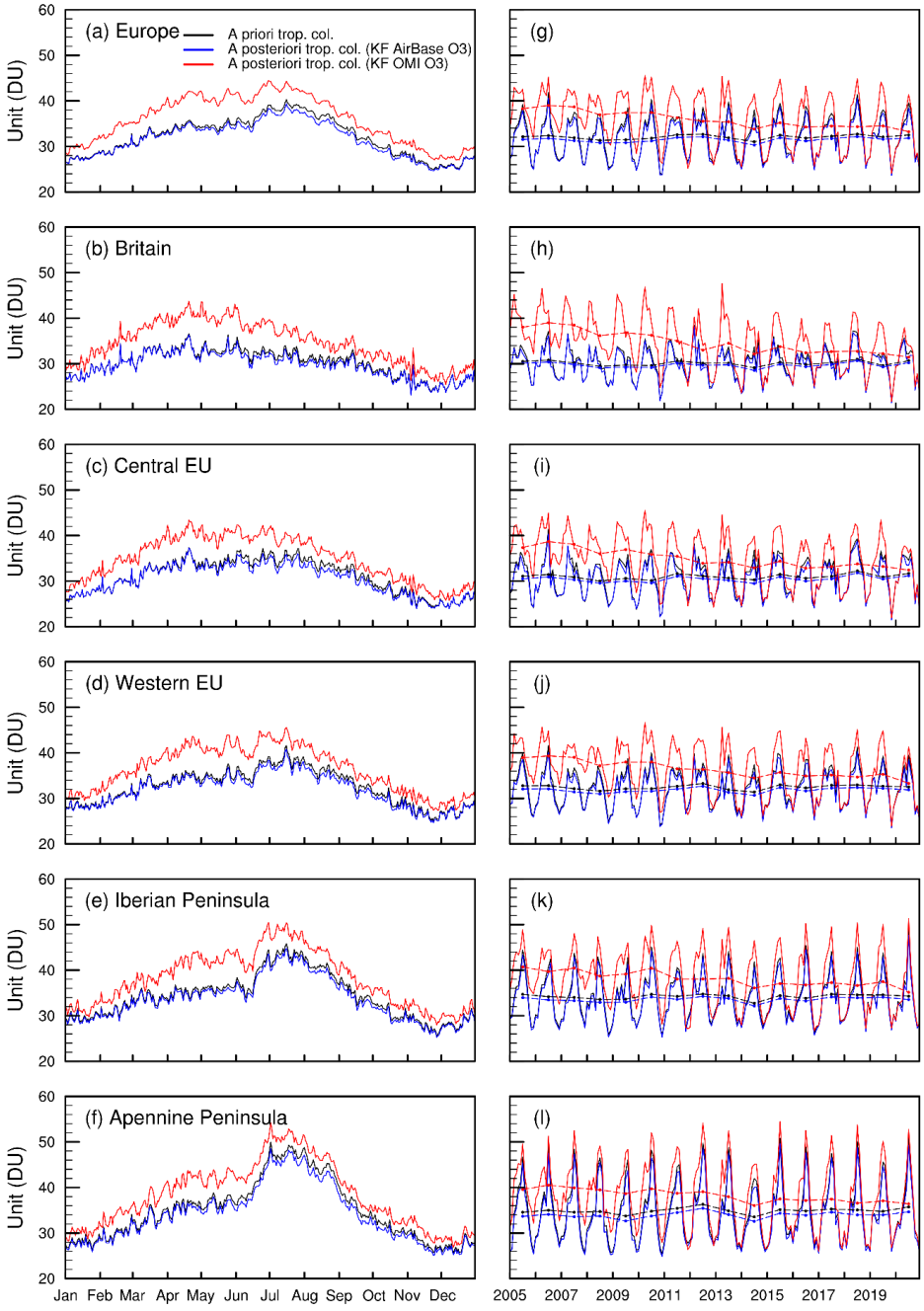

Fig. 10. (A-F) Daily averages of tropospheric O_3 columns over Europe in 2005-2020 from GEOS-Chem a priori simulation (black) and a posteriori simulations by assimilating AirBase (blue) and OMI (red) O_3 observations. (G-L) Monthly averages of tropospheric O_3 columns. The dashed lines in panels G-L are annual averages.

https://doi.org/10.5194/acp-2023-47
Preprint. Discussion started: 17 April 2023

Atmospheric Chemistry and Physics Discussions

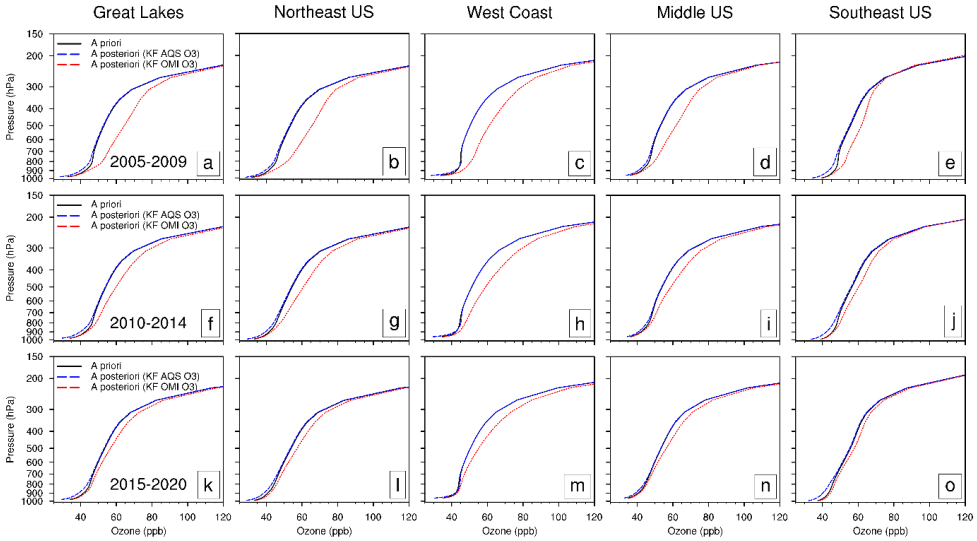

Fig. 11. Averages of O_3 vertical profiles in 2005-2020 in the US from GEOS-Chem a priori (black) and a posteriori simulations by assimilating AQS (blue) and OMI (red) O_3 observations.

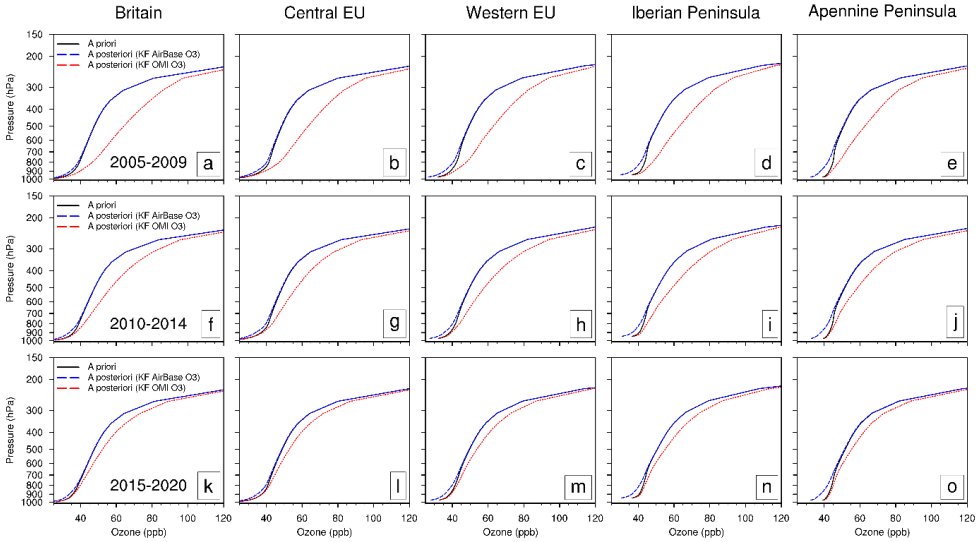

Fig. 12. Averages of O_3 vertical profiles in 2005-2020 in Europe from GEOS-Chem a priori (black) and a posteriori simulations by assimilating AirBase (blue) and OMI (red) O_3 observations.

https://doi.org/10.5194/acp-2023-47
Preprint. Discussion started: 17 April 2023

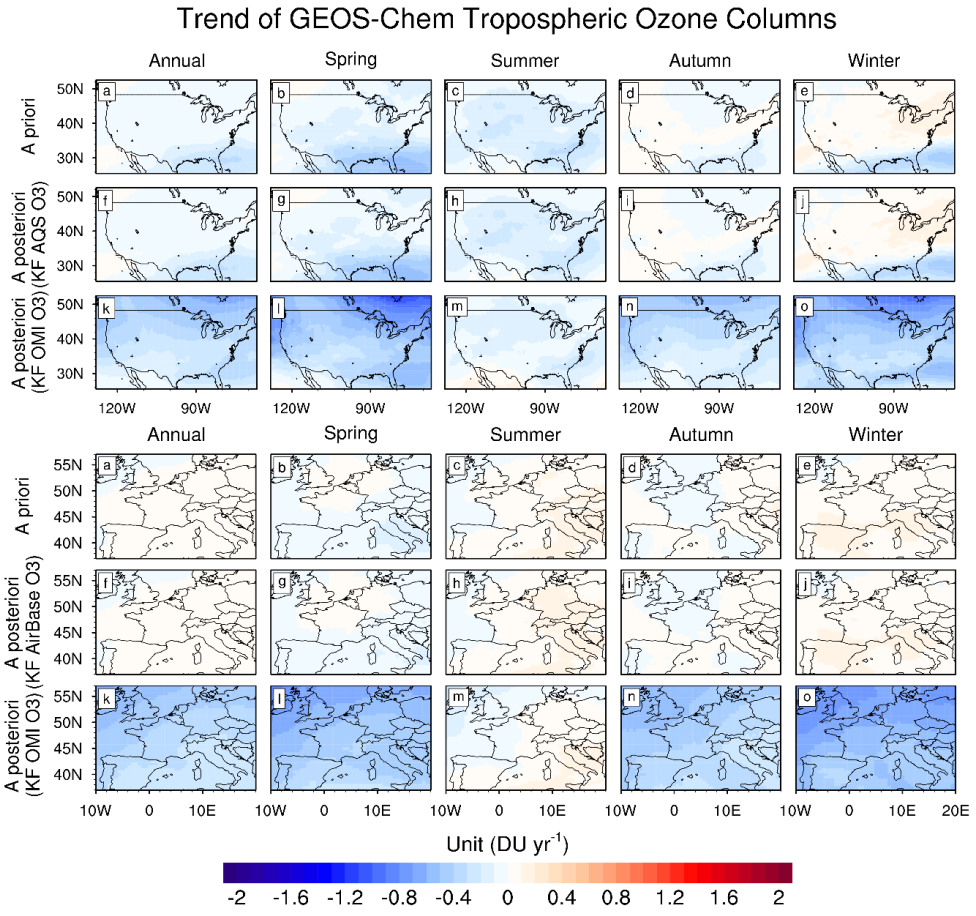

Fig. 13. Trends of tropospheric O_3 columns in 2005-2020 (annual and seasonal averages) from (A-E) GEOS-Chem a priori simulation; (F-J) assimilations of AQS or AirBase surface O_3 observations; (K-O) assimilations of OMI O_3 observations.